

193nm excimer laser inscribed Bragg gratings in microfibers for refractive index sensing

Yang Ran, Yan-Nan Tan, Li-Peng Sun, Shuai Gao, Jie Li, Long Jin,
and Bai-Ou Guan*

Institute of Photonics Technology, Jinan University, Guangzhou 510632, China
*iguanbo@jnu.edu.cn

Abstract: We demonstrate the inscription of fiber Bragg gratings by 193 nm ArF excimer laser in microfibers drawn from the standard single mode telecommunication fiber. Fiber Bragg gratings are directly inscribed in a series of microfibers with diameter ranged from tens of μm to $3.3 \mu\text{m}$ without hydrogen loading or other treatment to photosensitize the microfibers. Four reflection peaks are observed where three correspond to high order mode resonances. The resonance wavelength depends on the fiber diameter and it sharply blueshifts as the diameter is decreased below $10 \mu\text{m}$. The gratings are characterized for their response to ambient refractive index. The higher order mode resonance exhibits higher sensitivity to refractive index.

©2011 Optical Society of America

OCIS codes: (060.2310) Fiber optics; (060.2370) Fiber optics sensors; (230.3990) Micro-optical devices; (060.3735) Fiber bragg gratings.

References and links

1. L. M. Tong, J. Y. Lou, and E. Mazur, "Single-mode guiding properties of subwavelength-diameter silica and silicon wire waveguides," *Opt. Express* **12**(6), 1025–1035 (2004).
2. L. M. Tong, J. Y. Lou, R. R. Gattass, S. L. He, X. W. Chen, L. Liu, and E. Mazur, "Assembly of silica nanowires on silica aerogels for microphotonic devices," *Nano Lett.* **5**(2), 259–262 (2005).
3. J. Y. Lou, L. M. Tong, and Z. Z. Ye, "Dispersion shifts in optical nanowires with thin dielectric coatings," *Opt. Express* **14**(16), 6993–6998 (2006).
4. L. M. Tong, R. R. Gattass, J. B. Ashcom, S. L. He, J. Y. Lou, M. Y. Shen, I. Maxwell, and E. Mazur, "Subwavelength-diameter silica wires for low-loss optical wave guiding," *Nature* **426**(6968), 816–819 (2003).
5. M. Sumetsky, "Uniform coil optical resonator and waveguide: transmission spectrum, eigenmodes, and dispersion relation," *Opt. Express* **13**(11), 4331–4340 (2005).
6. M. Sumetsky, Y. Dulashko, and A. Hale, "Fabrication and study of bent and coiled free silica nanowires: Self-coupling microloop optical interferometer," *Opt. Express* **12**(15), 3521–3531 (2004).
7. X. S. Jiang, Q. H. Song, L. Xu, J. Fu, and L. M. Tong, "Microfiber knot dye laser based on the evanescent-wave-coupled gain," *Appl. Phys. Lett.* **90**(23), 233501 (2007).
8. F. Xu, P. Horak, and G. Brambilla, "Optical microfiber coil resonator refractometric sensor," *Opt. Express* **15**(12), 7888–7893 (2007).
9. W. Liang, Y. Huang, Y. Xu, R. K. Lee, and A. Yariv, "Highly sensitive fiber Bragg grating refractive index sensors," *Appl. Phys. Lett.* **86**(15), 151122 (2005).
10. A. Iadicicco, S. Campopiano, A. Cutolo, M. Giordano, and A. Cusano, "Refractive index sensor based on microstructured fiber Bragg grating," *IEEE Photon. Technol. Lett.* **17**(6), 1250–1252 (2005).
11. A. N. Chryssis, S. M. Lee, S. B. Lee, S. S. Saini, and M. Dagenais, "High sensitivity evanescent field fiber Bragg grating sensor," *IEEE Photon. Technol. Lett.* **17**(6), 1253–1255 (2005).
12. X. Z. Sang, C. X. Yu, T. Maytevarunyoo, K. Wang, Q. Zhang, and P. L. Chu, "Temperature-insensitive chemical sensor based on a fiber Bragg grating," *Sens. Actuators B Chem.* **120**(2), 754–757 (2007).
13. A. N. Chryssis, S. S. Saini, S. M. Lee, H. Yi, W. E. Bentley, and M. Dagenais, "Detecting Hybridization of DNA by Highly Sensitive Evanescent Field Etched Core Fiber Bragg Grating Sensors," *Quantum Electron.* **11**(4), 864–872 (2005).
14. X. Fang, C. R. Liao, and D. N. Wang, "Femtosecond laser fabricated fiber Bragg grating in microfiber for refractive index sensing," *Opt. Lett.* **35**(7), 1007–1009 (2010).
15. Y. Zhang, B. Lin, S. C. Tjin, H. Zhang, G. H. Wang, P. Shum, and X. L. Zhang, "Refractive index sensing based on higher-order mode reflection of a microfiber Bragg grating," *Opt. Express* **18**(25), 26345–26350 (2010).

16. G. Brambilla, F. Xu, and X. Feng, "Fabrication of optical fibre nanowires and their optical and mechanical characterisation," *Electron. Lett.* **42**(9), 517–518 (2006).
 17. F. Bilodeau, B. Malo, J. Albert, D. C. Johnson, K. O. Hill, Y. Hibino, M. Abe, and M. Kawachi, "Photosensitization of optical fiber and silica-on-silicon/silica waveguides," *Opt. Lett.* **18**(12), 953–955 (1993).
 18. J. Albert, B. Malo, K. O. Hill, F. Bilodeau, D. C. Johnson, and S. Theriault, "Comparison of one-photon and two-photon effects in the photosensitivity of germanium-doped silica optical fibers exposed to intense ArF excimer laser pulses," *Appl. Phys. Lett.* **67**(24), 3529–3531 (1995).
 19. J. Albert, M. Fokine, and W. Margulis, "Grating formation in pure silica-core fibers," *Opt. Lett.* **27**(10), 809–811 (2002).
-

1. Introduction

In recent years microfibers have attracted a great attention owing to its superiority in providing high fraction of evanescent fields, low loss through extreme bends, manageable large waveguide dispersion, high nonlinearity, good compatible to conventional fibers as well as compact and flexible structure [1–4]. In sensing area, a large evanescent field of microfibers offers a good opportunity in detecting the refractive index (RI) of external environment with a high sensitivity [5–9].

Fiber Bragg grating (FBG) is one of the most important photonic sensing elements that have found a variety of applications. The advantages of FBG sensors include small size, wavelength encoding, and multiplexing capability. However, a typical FBG cannot be used for evanescent field sensing because the resonant coupling between forward and backward core modes is hardly influenced by ambient RI.

Combining FBGs and microfibers provides a platform for the development of RI sensors based on FBGs. Initially, researches focused on the method of etching conventional FBG to micrometer scale by hydrofluoric acid etching [10–13]. However, etching of fiber results in the degradation of the structure and mechanical property. Most recently, inscription of FBGs in the fibers that have been drawn to micrometer scale was demonstrated. X. Fang *et al.* reported FBGs fabricated in microfiber by the use of 800 nm femtosecond laser [14], where the grating was formed by physical damage of the microfibers. Due to the small diameter of microfibers, this physical damage makes microfibers fragile. Y. Zhang *et al.* reported FBGs fabricated in microfiber by the use of a 248 nm KrF excimer laser [15]. A microfiber drawn from single mode fiber almost loses its photosensitivity to ultraviolet exposure because the Ge-doped region becomes very tiny. To overcome this problem, in [15] a specially designed fiber with a Ge/B-codoped photosensitive inner cladding was used as raw material to maintain the photosensitivity, and extra hydrogen loading was performed to enhance the photosensitivity, which significantly increases the cost and difficulty of the fabrication of FBGs in microfibers.

In this paper, we present the inscription of FBGs in microfibers using 193 nm ArF excimer laser. The microfibers were drawn from the standard single mode telecommunication fiber. FBGs were directly inscribed in a series of microfibers with diameter ranged from tens of μm to 3.3 μm without hydrogen loading or other treatment to photosensitize the microfibers. The RI sensitivity of the FBGs in microfibers was characterized.

2. Fabrication of Bragg gratings in microfibers

The microfibers were fabricated from the standard single mode telecommunication fiber by flame-heated taper drawing approach. A 2-mm width flame generated by the burning of butane was used as the heat source. The microfibers with different diameters were fabricated by elongating the fiber along the axis with different speed rates. The microfibers were treated with the post-fabrication flame brushing by couple of seconds before the grating inscription. This treatment not only is helpful for achieving low loss and good noise suppression but also is capable to solve the degradation and surface contamination of microfiber during the preservation [16]. Enhancement of photosensitivity by flame brushing was reported, which usually needs a 1700°C flame and 20-minutes treatment [17]. In our experiment, this effect

can be ignored. Figure 1 shows the microscope images of some of the fabricated microfibers with different diameters.

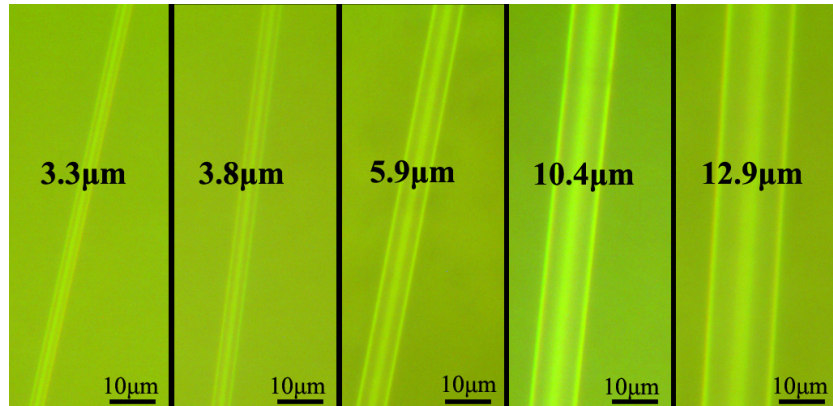


Fig. 1. Microscope images of the fabricated microfibers with different diameters.

FBGs were inscribed in the microfibers using a 193 nm ArF excimer laser and a phase mask with a period of 1089.2 nm. The microfiber was put in front of the phase mask with a distance of ~ 100 μm . The energy and repetition rate of the laser were set to 4 mJ/pulse and 200 Hz, respectively. A cylindrical lens was used to focus the UV beam to enhance the energy density. The energy density incident upon the microfiber was estimated to be 160 mJ/cm². Owing to the high efficiency associated with two-photon excitation process at 193 nm [18, 19], hydrogen loading or other photosensitization treatment were not needed, and FBGs were directly inscribed in the microfibers.

FBGs have been successfully inscribed in a series of microfibers with diameters of 83 μm , 63 μm , 18.5 μm , 12.9 μm , 10.4 μm , 5.9 μm , 3.8 μm , and 3.3 μm . The length of the FBGs was 3 mm, which is determined by the laser beam size. Figure 2 shows the typical transmission and reflection spectra of a FBG in microfiber with diameter of 10.4 μm . From the reflection spectrum, four resonance peaks at 1570 nm, 1561 nm, 1553 nm, and 1546 nm were observed. By calculating the effective refractive index of each linear polarization mode of the 10.4 μm microfiber, these four peaks can be attributed to resonance couplings from the forward fundamental mode to the backward LP01 (fundamental mode), LP21, LP12, and LP22 mode, respectively. The grating wavelength shifted toward the red part of the spectrum during the grating inscription process. This means that the grating formed in the microfiber was type I grating. Different from FBGs in microfibers inscribed by 248 nm excimer laser in [15], where only one high order mode resonance was observed because the index modulation is only induced in the Ge-doped photosensitive core region, the 193nm excimer laser produces index modulation in both the core and the cladding region, so higher order mode resonances are more easily excited.

Figure 3 shows the reflection spectra of Bragg gratings in the microfibers with diameters of 12.9 μm , 5.9 μm , 3.8 μm , and 3.3 μm , respectively. High-order-mode peaks were also observed for the FBGs in the 12.9 μm and 5.9 μm microfibers. The high-order-mode peaks of FBGs in the 3.8 μm and 3.3 μm microfibers shift out of the monitoring wavelength range and hence do not appear in Fig. 3(c) and 3(d). We theoretically predict that the LP21 mode resonance peak of FBG in the 3.3 μm microfiber is located at ~ 1450 nm. Figure 4 shows the measured and calculated Bragg wavelength (resonance wavelength of the fundamental mode) as a function of the microfiber diameter. The experimental data agree well with the theoretical expectation. In the simulation, the refractive index of the fiber core and the fiber cladding was set to 1.44922 and 1.44402, respectively, based on the typical data of standard single mode telecommunication fiber. Material dispersion was not taken into consideration in the

calculation. It can be seen from Fig. 4 that, with the decrease of the microfiber diameter, the Bragg wavelength shifts to shorter wavelength. This is because the fundamental mode energy expands to the silica cladding and then partially into the air, as the fiber is drawn from 125 μm to tens of microns, and then into several microns. As a result, the modal effective index decreases with the reduction of fiber diameter. The Bragg wavelength changes dramatically with diameter when the fiber diameter is below 10 μm due to the large refractive index difference between the thin silica core and the air cladding. In Fig. 3(d), the reflection peak exhibits a chirped characteristic with spectral bandwidth of ~ 6 nm, which reflects a certain nonuniformity in fiber diameter along the grating. This bandwidth corresponds to a diameter variation of 0.13 μm over the FBG, estimated from the calculated curve in Fig. 4. This result demonstrates the capability to measure the diameter uniformity for a microfiber through FBG inscription.

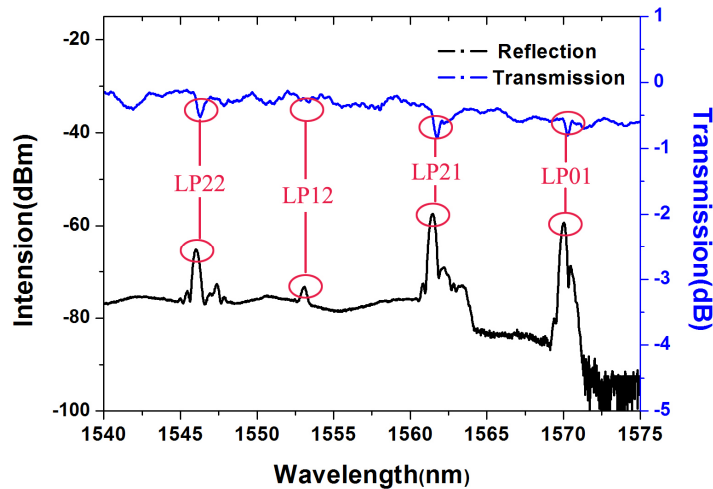


Fig. 2. Transmission and reflection spectra of the Bragg grating in the 10.4 μm microfiber.

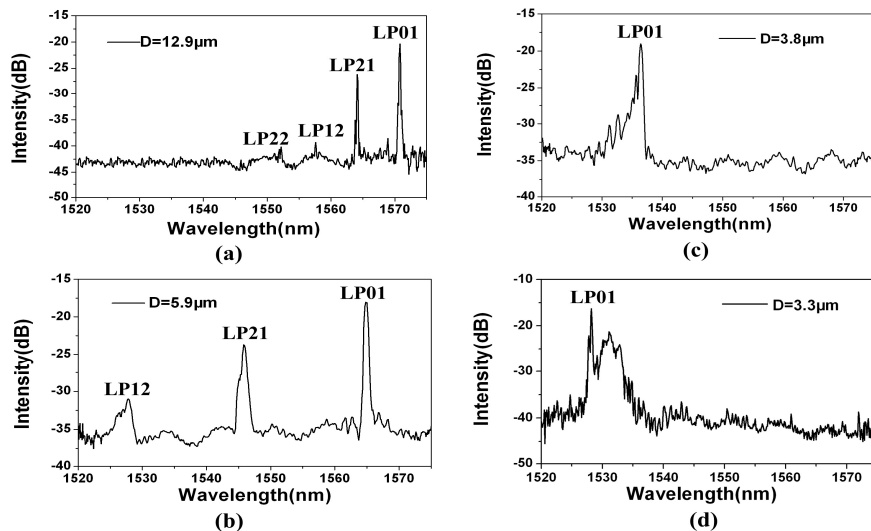


Fig. 3. Reflection spectra of FBGs in microfibers with diameter of (a) 12.9 μm , (b) 5.9 μm , (c) 3.8 μm , and (d) 3.3 μm .

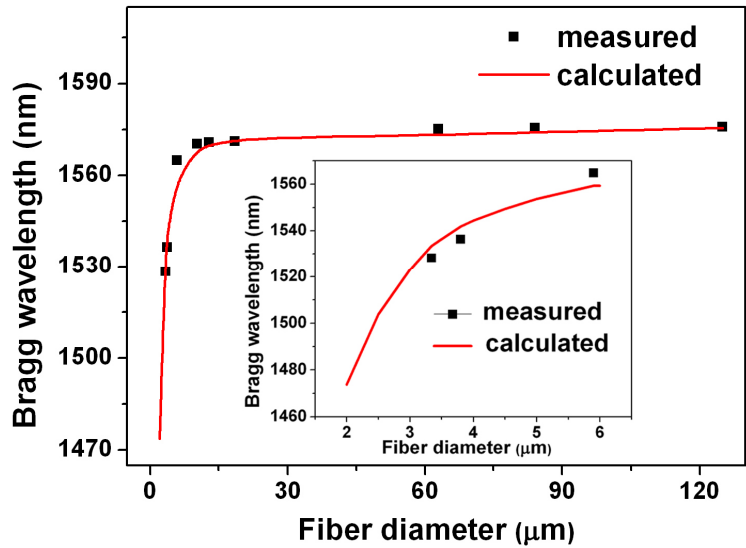


Fig. 4. Bragg wavelength versus the fiber diameter.

3. Response to refractive index

The response of the FBGs in microfibers to the ambient RI was characterized by immersing the FBGs into the sucrose solution. The RI was changed in range from 1.33 to 1.44 by changing the solution concentration. The reflection spectrum of the FBGs in microfibers was monitored with an optical spectrum analyzer (OSA) with resolution set to 0.01 nm.

Figure 5 shows the reflection spectra of a FBG in the 10.4 μm microfiber recorded in solution with different RI. When the FBGs were moved from air (RI≈1) into the sucrose solution, the grating resonance peaks experienced an abrupt shift to longer wavelength and the strength of the resonance peaks decreased. This is because the much higher RI of the sucrose solution compared to the air increases the effective index of the microfibers and hence enhances the evanescent wave propagating outside the microfiber.

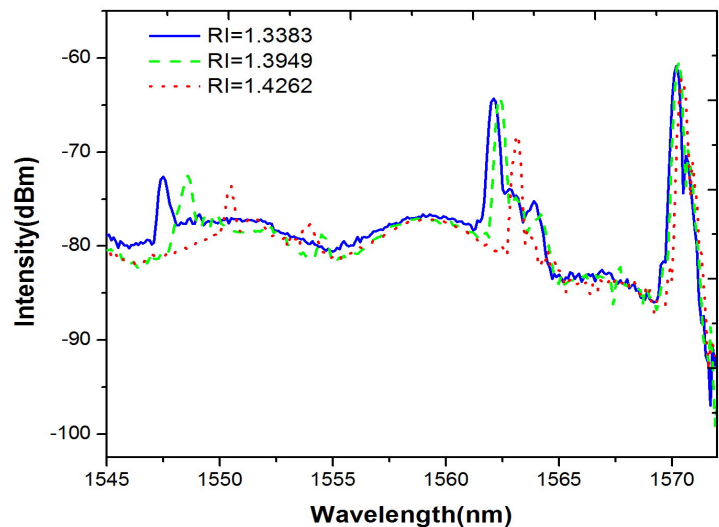


Fig. 5. Reflection spectra of the FBG in the 10.4 μm microfiber in different ambient RI.

The higher-order mode peaks demonstrate higher RI sensitivity because they have larger energy fractions outside the microfiber and therefore stronger interaction with the ambient RI is enabled. The relationship between the peak wavelengths and RI was plotted in Fig. 6(a). Because the LP12 resonance peak disappeared when the FBG was immersed into the solution, only the LP01, LP21 and LP22 resonance peaks were recorded. The experimental data in Fig. 6(a) can be fitted by the quadratic polynomial regression with $R > 99\%$. For comparison, the simulated wavelength variations are also plotted in Fig. 6(a), in agree with the experimental data. Figure 6(b) shows the fitted response sensitivity of different peaks as functions of RI. The sensitivity of the LP22 peak is about 92 nm/RIU at RI of 1.42.

The effect of the fiber diameter on the RI sensitivity was also investigated. Only the fundamental peak was recorded, since the high order peaks of the FBGs in the 3.8 μm and 3.3 μm microfiber were not in the monitoring wavelength range. The results were plotted in Fig. 7. It is clear that, the FBGs in thinner microfiber exhibits higher RI sensitivity. The RI sensitivity of the fundamental mode of the FBGs in the microfibers with diameter of 10.4, 3.8, and 3.34 μm was 9.5, 113.4, and 165 nm/RIU, respectively, at RI of 1.42. According to the simulation, the LP21 peak of the FBG in the 3.3 μm microfiber, which appears at 1450 nm, can reach ~ 600 nm/RIU at RI of 1.42.

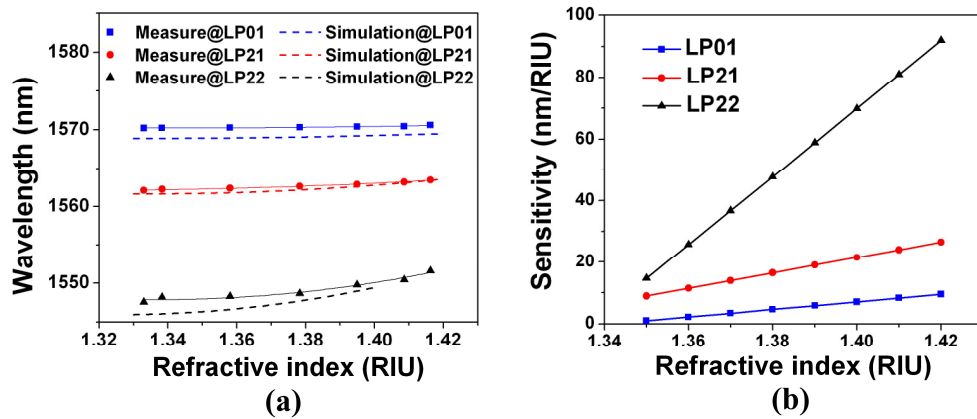


Fig. 6. (a) Measured and simulated RI response of the LP01, LP21, and LP22 peak of FBG in the 10.4 μm microfiber: (a) resonance wavelength versus RI; (b) sensitivity versus RI.

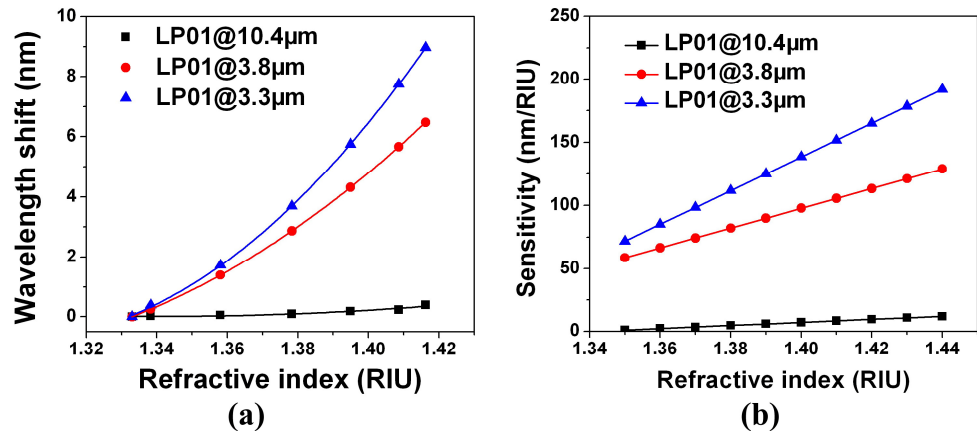


Fig. 7. (a) Relationships between wavelength shift and RI for FBGs in microfiber with different diameter; (b) RI sensitivities of FBGs in microfibers with different diameter.

4. Conclusion

The inscription of fiber Bragg gratings in microfibers by the use of 193 nm ArF excimer laser has been demonstrated. The microfibers were drawn from the standard single mode telecommunication fiber with the flame-heated drawing method. FBGs were directly inscribed in a series of microfibers with diameter ranged from tens of μm to 3.3 μm without hydrogen loading or other treatment to photosensitize the microfibers. The grating wavelength dramatically blueshifts with diameter as the microfiber diameter is below 10 μm . Four reflection peaks are observed where three correspond to high order mode resonances. The RI sensitivity of the FBGs depends on both the fiber diameter and the mode order. Thinner fiber and higher order mode result in higher RI sensitivity. The RI sensitivity of the LP01 peak and LP21 peak of the FBGs in microfiber with diameter of 3.3 μm was ~ 165 nm/RIU and estimated to be ~ 600 nm/RIU, respectively, at RI of 1.42.

Acknowledgements

This work was supported by National Natural Science Foundation of China (Grant No. 60736039 and 11004085) and the Fundamental Research Funds for the Central Universities (Grant No. 21609102).